12th AIAA/CEAS Aeroacoustics Conference (27th AIAA Aeroacoustics Conference)
8 - 10 May 2006, Cambridge, Massachusetts

AIAA 2006-2538

Influence of Vortex Core on Wake Vortex Sound Emission

Z. C. Zheng,[*] and Wenhua Li[†]

Kansas State University, Manhattan, Kansas 66506

F. Y. Wang[‡] and H. Wassaf[§]

USDOT John A. Volpe National Transportation Systems Center, Cambridge MA, 02142

A consistent and persistent mechanism of sound emission from aircraft wake vortices has been identified. Both measurement data and theoretical results show that a dominant frequency of sound pressure matches the rotation frequency of a Kirchhoff vortex due to the self-induction inside the vortex core. Numerical simulations for more realistic wake vortex pairs with inviscid ground effects and shear flow are carried out using a vortex particle method. A far-field vortex sound formulation, based on asymptotic expansions, is developed and compared with formulae in the literature. The simulation results reveal that the frequency of the wake sound emission would remain essentially the same as the classical Kirchhoff vortex, even under the influences of an inviscid ground effect or a weak-shear cross wind. The aforementioned results suggest that the mechanism identified should be fairly robust.

I.   Introduction

Fundamentally predicting aircraft wake vortices is one of the remaining challenges in unsteady, high Reynolds number fluid mechanics problems. Operationally, wake vortices pose both safety and capacity concerns. Wake encounters potentially could impose severe flight control demands in aircraft that are flying in limited airspace. The need to avoid such encounters is a primary consideration controlling aircraft spacing specifications around congested airports.[2,7] If the aircraft spacing specifications are too conservative, substantial reductions in passenger throughput result at busy airports. On the other hand, if the spacing standards are overly optimistic, potential dangerous vortex encounters can occur.

Previous efforts in the wake vortex research were concerned with developing engineering prediction models for the wake vortex behavior in response to weather conditions in the lower atmosphere.[4, 14, 42–44] More recently, a scheme for actively monitoring wake vortices has emerged by passively tracking the acoustic emissions from wake vortices.[15] This possibility is currently under examination. For that purpose, the key questions that need to be answered are: 1) Do wake vortices generate sound every time? 2) If so, is the generated acoustic signal consistent and measurable?

The answer to the first question should be positive from the point of view of fluid dynamics and aeroacoustics. This is because the flow related to wake vortices is highly unsteady: the unsteady motion of the vortices, vortex decay, vortex instabilities and breakdown, wake interactions with the ambient turbulence and stratification, ground effects, etc.. With all the unsteadiness, it would be really hard to keep wake

---

[*]Associate Professor, Department of Mechanical and Nuclear Engineering, AIAA Senior Member
[†]Graduate Research Assistant, Department of Mechanical and Nuclear Engineering
[‡]Aerospace Engineer, Advanced Communication, Navigation and Surveillance Division, RTV-4A, Senior Member AIAA.
[§]Electronics Engineer, Advanced Communication, Navigation and Surveillance Division, RTV-4A.

American Institute of Aeronautics and Astronautics

vortices quiet. With various scales at which these multiple vortices interact with each other, it may also be anticipated that the measured acoustic spectra emitted from the trailing wake would be of broadband in nature.

Now the difficult part is the second question. The airspace around an airport is a quite noisy environment. Noise sources include those from engines, airframes and the atmosphere (such as wind noise), in addition to all the vortex wakes from airplanes in the terminal area air traffic. Therefore, the second question should be answered from the perspective of what is unique to the wake vortex sound, in both the signal patterns and source mechanisms, as well as in the relation between the two. In terms of source mechanisms, all the above mentioned unsteady flow structures have unique aspects pertaining to wake vortices. However, not all of them can generate a reliable, repeatable and detectable acoustic signal. The studies to date have focused on experimental characterization,[3, 5, 9, 12, 24, 31, 32, 36] and a rigorous analytical identification of the noise source that is consistent and unique to aircraft vortices is lacking. We have started theoretical investigations on some of the scenarios targeting at identifying the consistent wake noise source.

There are only two possible ways to make a vortex system to emit sound: unsteady motion of the vortices, or change of strength.[30] The internal decay of a vortex due to viscous and turbulent effects is a very slow process in a realistic high-Reynolds-number environment, such as the environment for the aircraft wake vortex system. With external influences such as background turbulence and stratification, the decay process can be sped up[13] and, at the same time, be oscillatory. A previous study shows that the related sound emission can peak at a frequency that is dependent to the circulation fluctuations and the vortex decay coefficient.[40] Because of the low frequency nature of the background turbulence and stratification, this probably provides a possible mechanism for broadband, low frequency vortex sound emission. However, field measurement data showed higher frequency contents of sound from an aircraft wake vortex,[24] even when the vortex is out of ground effect.

This research is intended to identify a higher frequency source in an isolated vortex system that includes out-of-ground aircraft wake vortices and wake vortices in inviscid ground effects. While the currently identified decay mechanisms only produce low-frequency sound, the higher frequency emission source is thus attributed to the unsteady vortex motion. Tang and Ko[34, 35] identified two independent types of unsteady vortex motion that represent contributions to the sound source: the vortex centroid dynamics and the microscopic vortex core dynamics. Their analysis showed that the vortex core deformation intends to generate higher-frequency sound than the vortex centroid dynamics. Tang and Ko[34, 35] and others[11, 17, 18] focused their studies on vortex systems where the unsteady vortex motions are due to leapfrogging, collision, or coalescence. These types of vortex interactions rarely happen in a fully developed aircraft vortex wake, probably not until the Crow instability[8] occurs which leads to demise of wake vortices. Therefore during the life time of a longevity wake vortex system, the primary vortex-core dynamics is not driven by any of the above interactions. Rather, the unsteady core dynamics is due to the initial eccentricity during the roll-up process, the influence from the background shear, or the ground boundary effect. Addressing these issues is the concentration of the current study. A Kirchhoff spinning-core vortex[23] model is thus used as a starting point.

There may exist interactions between the wake vortex systems and the ambient turbulence that can sometimes be modeled as a primary vortex structure interacting with a secondary vortex structure. The ground effect, who possibly causes very low-frequency sound emission with the vortex translational acceleration in an inviscid manner,[15] is still able to produce complex unsteady fluctuations due to boundary-layer separation and thus needs to be considered. Compressibility can also contribute to the vortex core dynamics.[11] In addition, sinusoidal and eigen-oscillation instabilities can also occur in the short wave form[22, 33, 39, 41] whose wavenumber can be up to 8 times that of the Crow instability. But the associated sound is also of lower frequency than that observed experimentally. These effects on vortex sound emission will be tackled in another study.

In this study, a vortex particle method[6] is used to simulate the vortex core dynamics in two-dimensional, inviscid and incompressible flow. This is particularly suitable for a wake vortex system that is slowly-varying in the axial direction, and is high Reynolds number and low Mach number in nature. A far-field

American Institute of Aeronautics and Astronautics

vortex sound formula based on matched asymptotic expansions is used to relate sound emission to the vortex core dynamics.

II.   Sound Emission from a Spinning Kirchhoff Vortex Core

The Kirchoff vortex is a patch of constant vorticity inside an ellipse and zero vorticity outside. It is an exact solution of the two-dimensional, incompressible and inviscid flow equations.[23] An almost circular Kirchhoff vortex has the ellipse defined by the polar equation

$$r = a[1 + \epsilon \cos(2\theta - \Omega t/2)] \, , \tag{1}$$

where the long axis of the ellipse is $a(1 + \epsilon)$, the short axis is $a(1 - \epsilon)$, $\epsilon \ll 1$, and Ω is the uniform vorticity in the core. Howe[16] gave the acoustic pressure at $\Omega r/c_o \to \infty$ as

$$p = -\frac{\epsilon}{8} \sqrt{\frac{2\pi a}{r}} \rho_o U^2 M^{3/2} \cos[2\theta - \frac{\Omega}{2}(t - \frac{r}{c_o} + \frac{\pi}{4})] \, , \tag{2}$$

where $U = a\Omega/2$ and $M = U/c_o$. The ellipse rotates at an angular velocity of $\Omega/4$, which generates a quadrupole-type sound at a frequency of $\Omega/4\pi$, as shown in Eq. (2). Equation (2) also shows that for $\epsilon = 0$, which is the case of a circular vortex patch in an unbounded potential flow, e.g. a Rankine vortex,[33] there is no emission because of the steady-state flow produced by a Rankine vortex. In the wake vortex system, the eccentricity can be produced during the initial roll-up process. That a vortex resulted from shear layer instability is elliptical is an evidence. Other external effects such as wind shear or turbulence can also deform a circular vortex.

The analytical solution for the flow field of the Kirchhoff vortex is used to verify the results from the vortex particle method used in this study, and Eq. (2) is used as a base model to estimate sound emission frequencies from different types of aircraft and to verify the results from the far-field vortex sound formula presented in the next section.

III.   Far-Field Sound Formula for a Discrete Vortex System

A matched-asymptotic-expansion method[20,40] is used that matches the inner region of incompressible flow to the outer region of acoustic field. However, in the previous research, only were the dipole-type acoustic sources concerned, while in the vortex core problem, only is quadrupole noise generated as in Eq.(2). Therefore a higher order expansion than those previously derived[20,40] is needed for the near field. The inner region flowfield is generated by a system of discrete vortices, with the complex velocity potential expressed as

$$W = \Phi + i\Psi = \frac{i}{2\pi}\Gamma_j(t) \ln[z - z_j(t)] \, , \tag{3}$$

where Γ_j is the jth vortex circulation at position z_j, and z is the far-field location. Both Γ_j and z_j can be functions of time. The Einstein summation convention, with respect to j, is implied. After expanding the logarithmic function in Eq. (3) under the condition of $|z_j/z| \ll 1$, we have

$$W = \frac{i}{2\pi} \ln z \sum_j \Gamma_j - \frac{i}{2\pi}\Gamma_j\frac{z_j}{z} - \frac{i}{4\pi}\Gamma_j\frac{z_j^2}{z^2} + O[(\frac{z_j}{z})^3] \, . \tag{4}$$

The first term does not relate to acoustic sources, and is steady following Kelvin's theorem. Denoting the fluctuation complex velocity potential as w, we have

$$w = -\frac{i}{2\pi z}\Gamma_j z_j - \frac{i}{4\pi}\Gamma_j\frac{z_j^2}{z^2} \, . \tag{5}$$

American Institute of Aeronautics and Astronautics

By means of the linearized Bernoulli equation, the inner pressure fluctuation is

$$p_i = -\frac{\partial \phi}{\partial t} = \frac{1}{2\pi r} \left[\frac{d(\Gamma_j x_j)}{dt} \sin\theta - \frac{d(\Gamma_j y_j)}{dt} \cos\theta \right] - \frac{1}{4\pi r^2} \left\{ \frac{d}{dt}[\Gamma_j (2xy)_j] \cos(2\theta) - \frac{d}{dt}[\Gamma_j (x_j^2 - y_j^2)] \sin(2\theta) \right\} ,$$
(6)

where $r = |z|$ and $\theta = Arg(z)$ are the distance and angle of the far-field receiver, respectively, and are assumed independent of time.

The pressure fluctuation at the outer region, p_o, satisfies the convective wave equation

$$\frac{\partial^2 p_o}{\partial x^2} + \frac{\partial^2 p_o}{\partial y^2} - M^2 \frac{D^2 p_o}{Dt^2} = 0 .$$
(7)

After transformation using the outer variables and letting $M \to 0$, the acoustic equation is obtained

$$\frac{\partial^2 p_o}{\partial X^2} + \frac{\partial^2 p_o}{\partial Y^2} - \frac{\partial^2 p_o}{\partial t^2} = 0 ,$$
(8)

where $X = Mx$ and $Y = My$. The format of the outer solution is suggested by the inner solution to be

$$p_o = \sum_j S_j(R,t) \sin\theta + \sum_j C_j(R,t) \cos\theta + \sum_j K_j(R,t) \cos 2\theta + \sum_j L_j(R,t) \sin 2\theta ,$$
(9)

where $R = Mr$, and S_j, C_j, K_j and L_j are functions to be determined. After substituting this expression into Eq. (8) and performing the Fourier transform in time, Eq. (8) can be solved to give p_o in the frequency domain for the out-going waves,

$$\hat{p}_o = (\sum_j A_j \sin\theta + \sum_j B_j \cos\theta)H_1^{(2)}(\omega R), +(\sum_j E_j \cos 2\theta + \sum_j G_j \sin 2\theta)H_2^{(2)}(\omega R),$$
(10)

where $H_1^{(2)}$ is the second kind Hankel function of order one, $H_2^{(2)}$ is the second kind Hankel function of order two, ω is the frequency and A_j, B_j, E_j and G_j are determined by the matching condition between the inner and outer solutions.

The matching is performed by letting $R \to 0$ in Eq. (10) and re-writing the expression in terms of the inner variables. Since

$$H_1^{(2)}(\omega R \to 0) \to \frac{2\text{i}}{\pi \omega R} = \frac{2\text{i}}{\pi \omega M r} ,$$
(11)

and

$$H_2^{(2)}(\omega R \to 0) \to \frac{4\text{i}}{\pi (\omega R)^2} = \frac{4\text{i}}{\pi \omega^2 M^2 r^2} ,$$
(12)

substituting these expressions into Eq. (10) and comparing with Eq. (6) yields the outer solution as

$$\hat{p}_o = -\text{i}\frac{M\omega}{4}H_1^{(2)}(\omega R) \sum_j \left\{ \mathbf{F}\left[\frac{d(\Gamma_j x_j)}{dt}\right] \sin\theta - \mathbf{F}\left[\frac{d(\Gamma_j y_j)}{dt}\right] \cos\theta \right\}$$

$$+\text{i}\frac{M^2\omega^2}{16}H_2^{(2)}(\omega R) \sum_j \left\{ \mathbf{F}\left[\frac{d(2\Gamma_j x_j y_j)}{dt}\right] \cos 2\theta - \mathbf{F}\left[\frac{d(\Gamma_j (x_j^2 - y_j^2))}{dt}\right] \sin 2\theta \right\} ,$$
(13)

where $\mathbf{F}[\ ]$ denotes the Fourier transform in time.

With only the quadrupole source from the vortex core, the dipole terms (related to $\sin\theta$ and $\cos\theta$) in Eq. (13) are zero. The strengths of the quadrupole terms depend on $\Gamma_j x_j y_j$ and $\Gamma_j (x_j^2 - y_j^2)$, a fact that agrees with those expressions for two-dimensional vortex systems by Mohring[26, 27] and others.[16, 21, 25, 34] Equivalency among these expressions is checked and discussed in Appendix.

IV. Case Studies for Out-of-Ground Vortex Wake without Background Flow

Table 1 lists the majority aircraft types and their configurations (related to the wake vortex behavior) whose wake vortex sound were measured during the 2003 phased array test at Denver International Airport.[9,36] The wake sound emission frequencies are calculated based on the Kirchhoff vortex model. The wake vortex span is estimated as 78.5% of the wing span according to a typical elliptical wing loading. The circulation is calculated approximately from a uniform aircraft landing weight at 80% maximum landing weight with fixed approach speed. While it is difficult to accurately estimate the vortex core size, a reasonable range of the core radius is from 1.5% to 2% wing span.[10] A median core radius in between this range is selected as 1.65% of wingspan. With the relation of $\Omega = \Gamma/a^2$, the acoustic frequency of a Kirchhoff single vortex can be calculated as $f = \Omega/4\pi$. The LB, Median and UB frequencies correspond respectively to the core radii of 2%, 1.65% and 1.5% wing span. The last column of Table 1 is the results of computational simulation for the wake vortices modeled as a pair of counter-rotating vortices initially as Kirchhoff vortices with a median core size (1.65% wing span). The simulation procedure is explained later. It can be seen in Table 1 that the acoustic frequencies from the numerical results are almost exactly the same as that predicted by a single Kirchhoff vortex model using Eq. (2). This is due to the fact that the mutual induction effect does not influence the vortex core rotating dynamics, a point shared by Tang and Ko[35] to be further explored later.

Aircraft Configuration and Wake Frequency

		Wing span b	Wake vortex span bo	Circulation Gamma	Min Core Radius- 1.5%b	Median Core Radius- 1.65%b	Max Core Radius- 2%b	LB Acoustic Freq. (single)	Median Acoustic Freq. (single)	UB Acoustic Freq. (single)	Half of vortex span L	Maximum rotating speed	Numerical Median Freq. (pair)
		(m)	(m)	(m^2/s)	(m)	(m)	(m)	(Hz)	(Hz)	(Hz)	(m)	(m/s)	(Hz)
Airbus	A318	34.15	26.82	252.68	0.51	0.56	0.68	13.72	20.16	24.40	13.41	71.38	20.20
	A319	34.15	26.82	265.77	0.51	0.56	0.68	14.43	21.21	25.66	13.41	75.08	21.25
	A320	34.15	26.82	274.72	0.51	0.56	0.68	14.92	21.92	26.53	13.41	77.61	21.96
	A321	34.15	26.82	266.76	0.51	0.56	0.68	14.49	21.29	25.76	13.41	75.36	21.33
	A343	60.06	47.17	458.12	0.90	0.99	1.20	8.04	11.82	14.30	23.59	73.58	11.84
Boeing	B717	28.35	22.27	235.57	0.43	0.47	0.57	18.56	27.26	32.99	11.13	80.14	27.31
	B737	28.96	22.75	281.74	0.43	0.48	0.58	21.27	31.25	37.81	11.37	93.83	31.31
	B738	34.45	27.06	262.06	0.52	0.57	0.69	13.98	20.54	24.86	13.53	73.37	20.58
	B757	38.11	29.93	347.95	0.57	0.63	0.76	15.17	22.29	26.97	14.97	88.07	22.33
	B767	47.56	37.35	377.17	0.71	0.78	0.95	10.56	15.51	18.77	18.68	76.49	15.54
	B777	60.67	47.65	456.62	0.91	1.00	1.21	7.86	11.54	13.97	23.83	72.60	11.56
MD	MD80	32.93	25.86	240.32	0.49	0.54	0.66	14.04	20.62	24.95	12.93	70.40	20.66
	MD90	32.93	25.86	276.26	0.49	0.54	0.66	16.14	23.71	28.69	12.93	80.93	23.75
Regional	B190	17.68	13.89	70.93	0.27	0.29	0.35	14.36	21.11	25.54	6.94	38.69	21.15
	CRJ2	21.04	16.52	139.14	0.32	0.35	0.42	19.91	29.25	35.40	8.26	63.80	29.31
	BA46	26.22	20.59	283.17	0.39	0.43	0.52	26.08	38.32	46.37	10.30	104.18	38.40
	DH8B	25.91	20.35	144.55	0.39	0.43	0.52	13.63	20.03	24.23	10.18	53.81	20.06
	E120	25.91	20.35	101.14	0.39	0.43	0.52	9.54	14.01	16.95	10.18	37.65	14.04

Table 1. Aircraft types and estimated frequencies based on the Kirchhoff vortex model.

The acoustic frequencies versus the wing span in Table 1 is plotted in Fig. 1. By grouping the aircraft types into small RJs and large jets, it shows that wake acoustics from large aircraft has an inverse relation between peak frequency and wing span. Small aircraft do not follow such a relation. Comparisons of this predicted trend with the field measurement data also provide evidences to confirm the relation for the large aircraft.
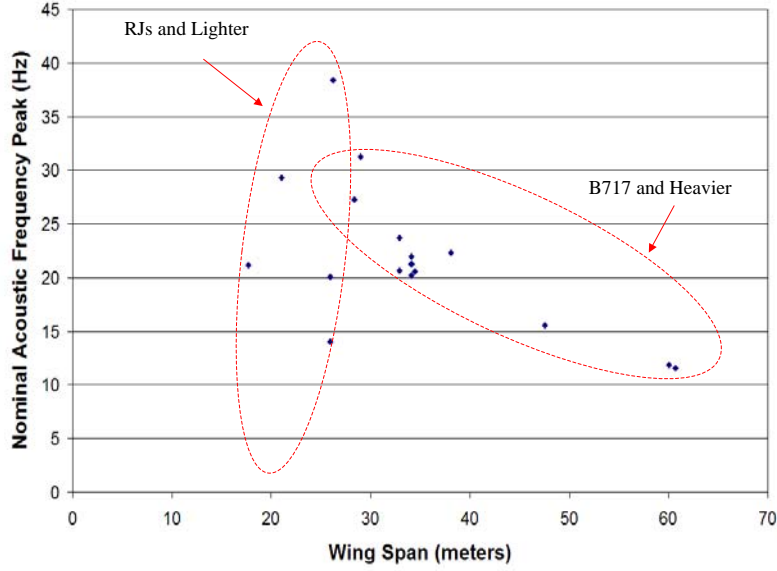
American Institute of Aeronautics and Astronautics

Figure 1. Acoustic frequencies versus the wing spans for different types of aircraft.

In Fig. 2, measured data are plotted for two cases of B737 and two cases of B757. Details of the measurement and data reduction procedure are described elsewhere.[37,38] In each case, there are three plots representing three units of non-dimensional time of measurement. In these measurements, one non-dimensional time unit is the approximate time for the vortex pair to descend one vortex span,[13] and is equal to $2\pi b_o^2/\Gamma$, where b_o and Γ are respectively the initial vortex span and circulation. Only the data from the second non-dimensional time (the middle plot in each figure) is used for comparison because it has the full time history of the measured data and is considered more accurate from the measurement point of view, although other two times are included for reference purpose. The blue and green lines represent background and wake vortex acoustic powers respectively. The red dots show the predicted frequency peaks based on the values in Table 1 for the median frequency values. The red vertical lines indicate the measured absolute peak, and the green vertical lines indicate the limit of the wake acoustic power detectable above background acoustic noise. Figure 2 shows the measured B757 wake peak frequencies are lower than those of B737, which confirms the trend predicted in the calculations based on the Kirchhoff vortex model. These circumstantial evidences suggest that the Kirchhoff vortex core should be the mechanism responsible for the peaks observed in the measured spectra. It should be pointed out that the comparisons of experimental results with the theory should focus on the trend, instead of the absolute values since the theoretical calculation requires input parameters that are very often not easily measured with high certainties of accuracy.

V. Numerical Simulation Cases

While the analytical solution of the Kirchhoff vortex is for a single vortex in an infinite domain, aircraft vortex wakes consist of a pair of counter-rotating vortices for which the analytical solution does not exist. In addition, ground effects and atmospheric conditions can further complicate the matter. Therefore, for realistic vortex wake cases, numerical solutions are needed and discussed in this section.
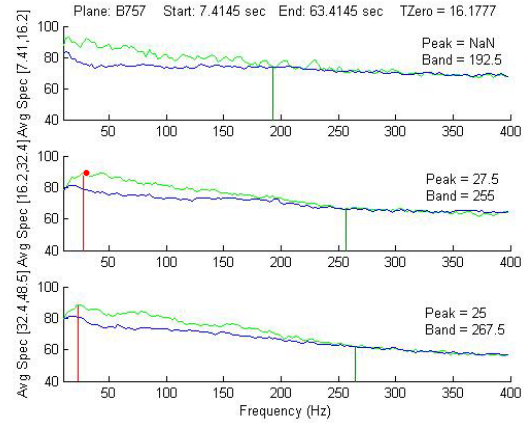
American Institute of Aeronautics and Astronautics
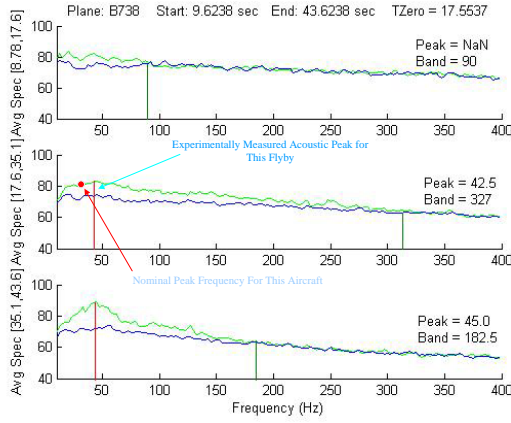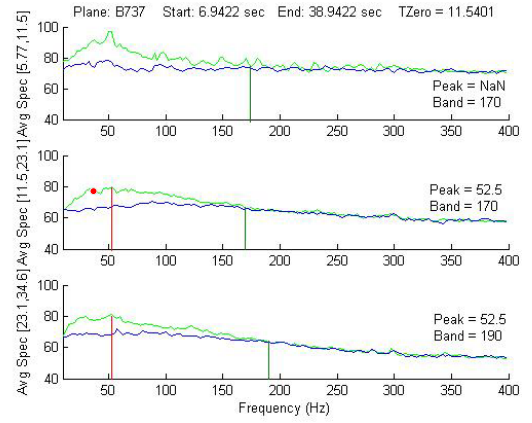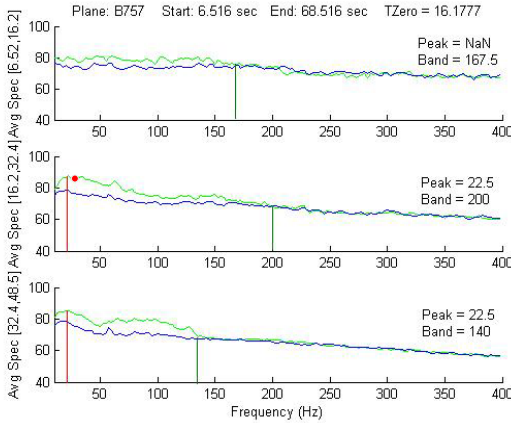
Figure 2. Measured wake acoustic spectra for B737 and B757, and comparisons of measured peak frequencies with the predicted frequencies using the Kirchhoff vortex model. (a) B737-800, (b) B737, (c) B757, (d) B757.

Using the vortex half-span as the characteristic length and the nominal maximum rotating speed at the outer edge of the vortex core, $a\Omega/2$, as the characteristic velocity, the simulation equations can be non-dimensionalized for computation purpose. The simulation procedure is developed using a vortex particle method.[6] At the beginning of the simulation, the initially specified Kirchhoff vortices have the parameters of $a = 0.042$, $\epsilon = 0.05$ and $\Omega = 47.69$, for the median core-size (1.65% wing span) vortices. The vortex particles are distributed on a grid mesh with the grid size of $\Delta x = \Delta y = 1.68 \times 10^{-3}$ and a particle core parameter α of $2\Delta x$.[11] This fine grid solution selected in the simulation is to ensure proper resolution for the vorticity field in order to correctly capture the core rotation frequency. Simulation tests with lower resolution have shown that the acoustic frequency numerically shifts to lower values. The required high resolution in this problem poses difficulties in using the Eulerian type of simulation in which only high-order accuracy schemes with high grid resolution are able to capture the frequency correctly.[29]

American Institute of Aeronautics and Astronautics

The initial distribution of vorticity is

$$\vec{\zeta}(\vec{x} - t) = \sum_n \Gamma_n g_\alpha(\vec{x} - \vec{x}_n(t)) \ , \tag{14}$$

where Γ_n is the circulation of each vortex particle defined as $(\Delta x)^2 \Omega$ in the Kirchoff vortex model here, and g_α is a second-order particle core function[6] defined as

$$g_\alpha(\vec{x}) = \frac{1}{\pi \alpha^2} \exp(-|\vec{x}|^2/\alpha^2) \ . \tag{15}$$

The size of time step is $\Delta t = 5.1465 \times 10^{-3}$, which is equal to $10T/512$, where T is the oscillation period of a single Kirchhoff vortex equal to $4\pi/\Omega$. By carrying out simulation of 512 time steps, a time history of 10 periods is covered. This time step is sufficiently small to resolve the frequency content related to the core vorticity in this case. During the simulation, re-meshing is done at each time step.

For modeling the wake vortex system, a counter-rotating vortex pair composed of two opposite-sign Kirchhoff vortices is used as the initial condition to represent the vortex wake out of ground effect. For in-ground-effect cases, an image pair of the wake vortices is placed at the other side of the ground boundary to represent the inviscid ground effect.

Figure 3 is an illustration (with exaggerated large vortex cores for easy discern and shown domain size truncated from the real domain used in the simulation) of the history of vorticity contours for a pair of out-of-ground wake vortices. It can be seen that it is the "churning" effect of the solid-body like rotation motion of the elliptical-shaped vortex cores that causes the unsteady fluid flow that is responsible for the far-field acoustics.
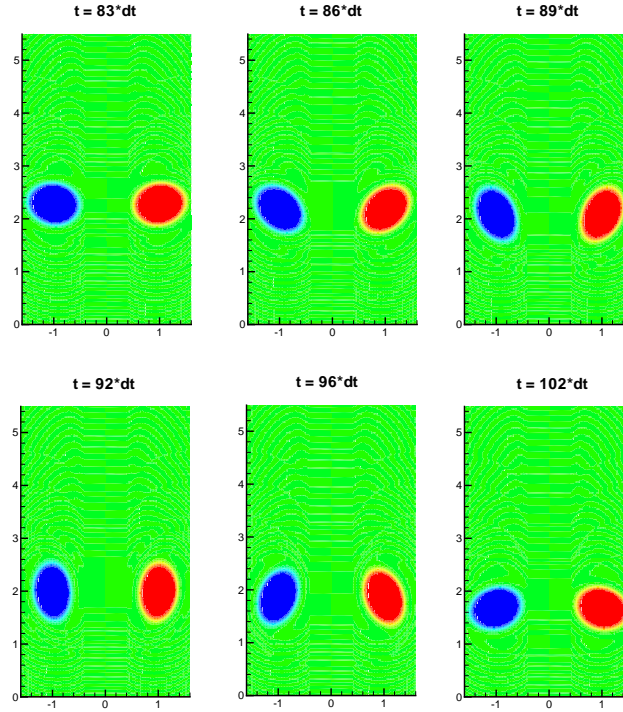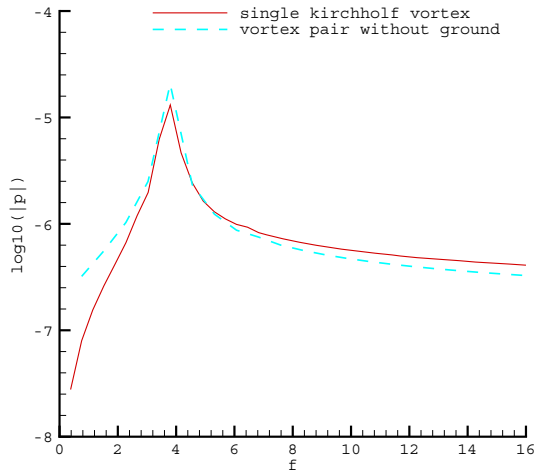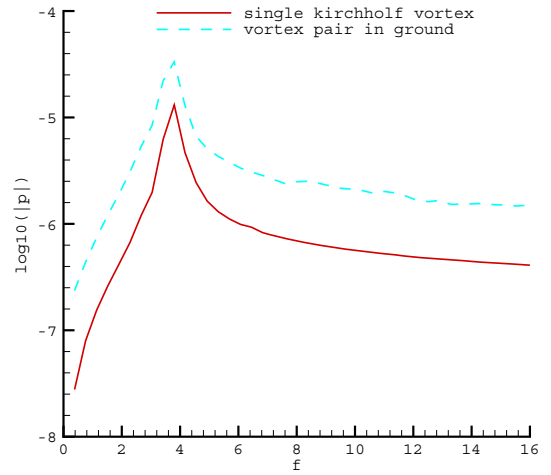

Figure 3. Illustration of the history of contours of the vortex wake represented by a pair of out-of-ground wake vortices initiated as a pair of counter-rotating Kirchhoff vortices.

American Institute of Aeronautics and Astronautics

(a)   (b)

Figure 4. (a) Comparison of the simulated spectrum of acoustic pressure between that of a single Kirchhoff vortex and that of a pair of counter-rotating vortices, (b) Comparison of the simulated spectrum of acoustic pressure between that of a single Kirchhoff vortex and that of a pair of counter-rotating vortices with the ground image.
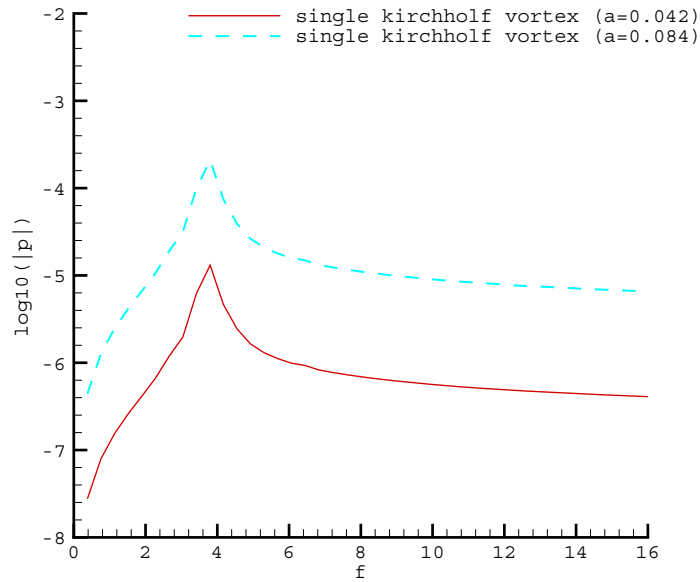

Figure 5. Comparison of simulated acoustic pressure spectra of two different core sizes of Kirchhoff vortices with the same vorticity value inside their cores.

American Institute of Aeronautics and Astronautics

Figure 4 compares the simulated spectrum of the far-field acoustic pressure calculated using Eq. (13). It should be noted that in several cases considered here, the second quadrupole term in Eq. (13), the $\Gamma_j(x_j^2 - y_j^2)$ term, turns out to be zero because of the vorticity symmetry in the flow field. However in other more general cases when the symmetry no longer exists, this term is not zero. Fig. 4(a) compares the single Kirchhoff vortex with the counter-rotating vortex pair, and Fig 4(b) compares the single Kirchhoff vortex with the counter-rotating vortex pair in ground effect. It can be seen that in all the cases, there exists a significant peak at the frequency of $f = 3.8$, which is exactly related to the vorticity value in the Kirchhoff vortex core as $\Omega/4\pi$, as shown in the analytical solution of Eq. (2). This means that the sound generation mechanism due to vortex core is independent of the type of the vortex interaction, as long as the straining field of the mutual induction is irrotational. This behavior of the vortex core mechanism agrees with a conclusion in Tang and Ko.[35]

Figure 5 is plotted to compare the effect of vortex core size. A case with an elliptical vortex core size of $a = 0.084$ is compared with the original core size of $a = 0.042$, with the same vorticity of 47.69 inside the core. It can be seen that the peak frequency still remains at $f = 3.8$. The magnitude of the spectrum is increased due to the increase of the core size with the same vorticity, because the total circulation, which is equal to the vorticity times the core area, is increased. This phenomenon agrees with what shows in Eq. (2), where the frequency of the acoustic pressure only depends on the vorticity level ($\Omega/2$), and the magnitude of the acoustic pressure is increased due to the increase of the core size a.

It is noted that under realistic atmospheric conditions, wind shear and turbulence, in the form of rotational straining field, can impose significant effects on the wake vortex core dynamics. There are several ways to simulate these effects. One way is to represent the background field with vorticity field and directly simulate the wake vortices along with the background vortices. While this method is able to directly simulate the interactions between background shear and the wake vortices, it is computationally expensive because a large number of vortices need to be distributed all over the computational domain to represent the background flow. Another way is to split the wake vortex flow from the background flow. Look, for example, at the vorticity transport equation for 2-D inviscid incompressible flow:

$$\frac{D(\overline{\Omega} + \Omega)}{Dt} = \frac{\partial(\overline{\Omega} + \Omega)}{\partial t}) + (\overline{u}_j + u_j)\frac{\partial(\overline{\Omega} + \Omega)}{\partial x_j} = 0 \;, \tag{16}$$

where the flow variables are split into the background flow $(\overline{\Omega}, \overline{u}_j)$ and the induced part by wake vortices (Ω, u_j). Neglecting the influence from wake vortices on background flow, the background flow itself satisfies

$$\frac{D\overline{\Omega}}{Dt} = \frac{\partial\overline{\Omega}}{\partial t} + \overline{u}_j\frac{\partial\overline{\Omega}}{\partial x_j} = 0 \;. \tag{17}$$

Substituting Eq. (17) into Eq. (16) results in

$$\frac{D\Omega}{Dt} = \frac{\partial\Omega}{\partial t} + (\overline{u}_j + u_j)\frac{\partial\Omega}{\partial x_j} = -u_j\frac{\partial\overline{\Omega}}{\partial x_j} \;. \tag{18}$$

If we only consider a constant-shear cross flow, this background flow satisfies Eq. (17). Since the background vorticity is constant, Equation (18) then becomes

$$\frac{D\Omega}{Dt} = \frac{\partial\Omega}{\partial t} + (\overline{u}_j + u_j)\frac{\partial\Omega}{\partial x_j} = 0 \;. \tag{19}$$

Therefore, the wake vortices can be treated as a pair of vortices transported at a velocity of background wind plus the induced velocity due to wake vortices. The vortex particle method can be easily implemented as

$$\frac{d\Gamma_p}{dt} = 0 \;, \tag{20}$$

American Institute of Aeronautics and Astronautics

$$\frac{d\vec{X}_p}{dt} = \overline{\vec{u}}_p + \vec{u}_p = \overline{\vec{u}}_p + \sum_q K_\alpha(\vec{X}_p - \vec{X}_q)\Gamma_q \ , \qquad (21)$$

where Γ_p and is the circulation of each vortex particle, and K_α is defined as

$$K_\alpha(\vec{X}) = \frac{\vec{X} \times \vec{k}}{2\pi|\vec{X}|}[1 - \exp(-|\vec{X}|^2/\alpha)] \qquad (22)$$

and the vortex particle core parameter, α, is selected in Eq. (15).

Figure 6 compares a case of a wake vortex pair in a background flow with constant shear with that of a single vortex. The vortices are initiated by the same parameters as mentioned before. The shear vorticity is 0.01. For a B757, this shear strength represents a crosswind speed increase of 0.06m/s per meter. Figure 6 shows again the dominant frequency remains to be that of the Kirchhoff vortex core rotation.

VI.   Conclusion

A consistent and persistent mechanism of sound emission from aircraft wake vortices has been identified. Both measurement data and theoretical results show that a dominant frequency of sound pressure matches the rotation frequency of a Kirchhoff vortex due to the self-induction inside the vortex core. Calculated results based on this mechanism using realistic aircraft configurations show that wake acoustics from large aircraft has an inverse relation between peak frequency and wing span. Small aircraft do not follow such a relation. By looking into a particular set of data for B757 and B737, both the measurement and the calculation agree that the B757 wake peak frequencies are lower than those of B737. When the wake vortices are initialized by a counter-rotating Kirchhoff vortices, numerical simulations based on the inviscid vortex particle method reveal that the frequency of the wake sound emission remains essentially the same as that of the classical Kirchhoff vortex, even under the influences of an inviscid ground effect and a weak-shear cross wind. These results suggest that the identified sound generation mechanism attributed to the vortex core dynamics should be a robust mechanism.
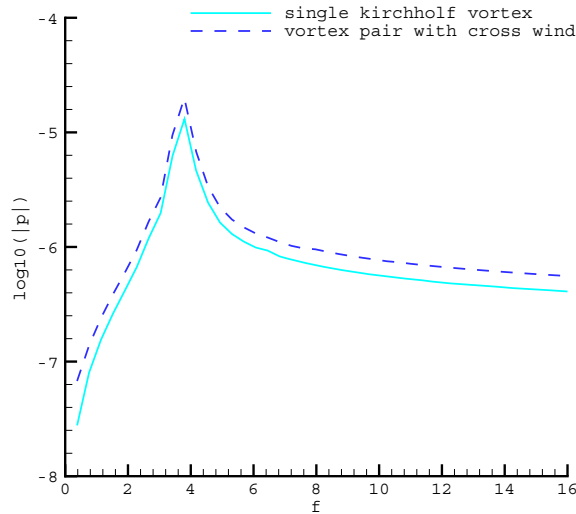

Figure 6. Comparison of acoustic pressure spectra of the wake vortex pair in a weak constant shear with that of a single Kirchhoff vortex.

Appendix

Mitchell et al.[25] presented a derivation of Mohring's two-dimensional quadrupole sound result[27] using the method of matched asymptotic expansions. That derivation followed the derivation of Mohring's three-dimensional result[26] given by Kambe et al.[19] Their result, in the frequency domain, is

$$\tilde{p}(\omega) = \frac{x_i x_j}{r^2} \frac{\rho_o \omega^3}{8c_o^2} \tilde{Q}_{ij} H_2^{(1)}(\frac{\omega r}{c_o}) \ , \tag{23}$$

where Q_{ij} is given by the second-order moments of vorticity

$$Q_{ij}(t) = \int (\vec{y} \times \vec{\Omega}(y,t))_i y_j dy^2 \ . \tag{24}$$

Note $\vec{x}$ and $\vec{y}$ are respectively far-field and near-field coordinates. This same expression was also obtained by Knio et al.[21] An expression for the time domain is given in Tang and Ko[34]

A more explicit form of Eq. (23) can be deduced as

$$\tilde{p}(\omega) = \frac{\rho_o \omega^3}{16c_o^2} H_2^{(1)}(\frac{\omega r}{c_o})[\tilde{Q}_1(\omega)\cos(2\theta) - \tilde{Q}_2(\omega)\sin(2\theta)] \ , \tag{25}$$

where the source terms Q_1 and Q_2, the second-order moments of vorticity, are

$$Q_1 = 2\int\int y_1 y_2 \Omega dy_1 dy_2 \ , \qquad Q_2 = \int\int (y_1^2 - y_2^2)\Omega dy_1 dy_2 \ . \tag{26}$$

On the other hand, the quadrupole term obtained in Eq. (13) can be re-written as

$$\tilde{p}(\omega) = -\frac{\rho_o \omega^3}{16c_o^2} H_2^{(2)}(\frac{\omega r}{c_o})(\tilde{Q}_1(\omega)\cos(2\theta) - \tilde{Q}_2(\omega)\sin(2\theta)) \ , \tag{27}$$

by noticing that

$$\mathbf{F}\left[\frac{d}{dt}\right] = \mathrm{i}\omega\mathbf{F}[\ ] \ .$$

It should be noted that the difference between our expression, Eq. (27), and the expression in the mentioned literature, Eq. (25), is due to the selection of the Hankel functions to ensure an out-going wave behavior of the acoustic pressure. A careful examination of the derivation procedures leading to each of the equations reveals that the difference is caused by the different definitions of the Fourier transform pair used in the two expressions. In our expression, the Fourier transform is defined as

$$F(\omega) = \int f(t)\exp(-\mathrm{i}\omega)dt \ , \qquad f(t) = \frac{1}{2\pi}\int F(\omega)\exp(\mathrm{i}\omega t)dt \ , \tag{28}$$

while in Eq. (25), the Fourier transform is defined as

$$F(\omega) = \int f(t)\exp(\mathrm{i}\omega)dt \ , \qquad f(t) = \frac{1}{2\pi}\int F(\omega)\exp(-\mathrm{i}\omega t)dt \ . \tag{29}$$

Therefore, the out-going wave branch uses different Hankel functions in the two expressions. In the near-field Eq. (27) and Eq.(25) become the same at $\omega r/c_o \to 0$ because[1]

$$H_2^{(2)}(\pm z) = \frac{4\mathrm{i}}{\pi z^2} = -H_2^{(1)}(\pm z) \ , \qquad z \to 0 \ , \tag{30}$$

so that they match to the same inner solution. The out-going wave behavior for each of Eq. (25) and Eq. (27) to match the two different definitions of the Fourier transform can be easily illustrated by looking at the Hankel function expressions at $\omega r/c_o \to \infty$.[1]

When they are transformed back to the time domain following each of their own definition of Fourier transform, Eqs. (25) and (27) should yield the same results. We now consider the example of a Kirchhoff vortex that has a uniform vorticity inside the Kirchhoff vortex core defined by a polar equation $R = a(1 + \epsilon cos(2\sigma - 0.5\Omega t))$, where σ is the near-field azimuthal angle. The source terms Q_1 and Q_2 can be calculated as

$$Q_1 = \Omega a^4 \epsilon \pi \sin(0.5\Omega t), \qquad Q_2 = \Omega a^4 \epsilon \pi \cos(0.5\Omega t). \tag{31}$$

By taking inverse Fourier transform and looking at the asymptotic behavior of the Hankel functions at $\Omega r/c_o \to \infty$, both Eqs. (25) and (27) give

$$p(t) = \frac{\epsilon}{8}\sqrt{\frac{2\pi a}{r}}\rho_0 U^2 M_0^{3/2} \cos(2\theta - 0.5\Omega t + \frac{\Omega r}{2c_0} + \frac{\pi}{4}). \tag{32}$$

There is a sign difference (a π phase difference) between this expression and Howe's[16] result, Eq. (2). It is noted that in Muller's[28] a sign difference is also mentioned.

Acknowledgments

References

[1] Abramowitz, M, and Stegun, I. A., *Handbook of Mathematical Functions*, Dover, New York, 1965.

[2] *Airman's Information Manual*, FAA, June, 1996.

[3] Alix, D. C., Simich, P. D., Wassaf, H., and Wang, F. Y., "Acoustic Characterization of Wake Vortices in Ground Effect," *43rd AIAA Aerospace Sciences Meeting and Exhibit*, AIAA Paper No. 2005-0260, Reno, NV, January 2005.

[4] Ash, R. L., and Zheng, Z. C., "Numerical Simulations of Commercial Aircraft Wakes Subjected to Airport Surface Weather Conditions," *Journal of Aircraft*, Vol. 35, No. 1, 1998, pp. 18-26.

[5] Booth, Jr., E. R. and Humphreys, Jr., W. M., "Tracking and Characterization of Aircraft Wakes Using Acoustic and Lidar Measurements," *11th AIAA/CEAS Aeroacoustics Conference*, AIAA-2005-2964, Monterey, CA, May 2005.

[6] Cottet, G.-H., and Koumoutsakos, P., *Vortex Methods, Theory and Practice*, Cambridge University Press, 2000.

[7] Critchley, J. B., and Foot, P. B., "United Kingdom Civil Aviation Authority Wake Vortex Database: Analysis of Incidents Reported between 1972 and 1990," *Proceedings of the FAA International Wake Vortex Symposium*, edited by J. N. Hallock, DOT/FAA/SD-92/1.1, Washington, DC, June, 1992, pp. 8-1-8-17.

[8] Crow, S. C., "Stability Theory for a Pair of Trailing Vortices," *AIAA Journal*, Vol. 8, 1970, pp. 2172-2179.

[9] Dougherty, R. P., Wang, F. Y., Booth, E. R., Watts, M. E., Fenichel, N. and D'Errico, R. E., "Aircraft Wake Vortex Measurements at Denver International Airport," *10th AIAA/CEAS Aeroacoustics Conference*, AIAA Paper No. 2004-2880, Manchester, UK, May 2004.

[10] Delisi, D. P., Greene, G. C., Robins, R. E., Vicroy, D. C., and Wang, F. Y., "Aircraft Wake Vortex Core Size Measurements," AIAA Paper AIAA-2003-3811, *21st AIAA Applied Aerodynamics Conference*, June 23-26, 2003, Orlando, FL.

[11] Eldredge, J. D., "The Acoustics of Two-Dimensional Leapfrogging Vortices," AIAA Paper 2005-2954, *11th AIAA/CEAS Aeroacoustics Conference*, May 23-25, 2005, Monterey, CA.

[12] Fine, N. E. and Kring, D.C., "Opto-Acoustic Tracking of Aircraft Wake Vortices," *11th AIAA/CEAS Aeroacoustics Conference*, AIAA-2005-2965, Monterey, CA, May 2005.

[13] Greene, G. C., "An Approximate Model of Vortex Decay in the Atmosphere," Journal of Aircraft, Vol. 23, No. 7, 1986, pp. 566-573.

[14] Han, J., Lin, Y., Arya, S. P., and Proctor, F. H., "Numerical Study of Wake Vortex Decay and Descent in Homogeneous Atmospheric Turbulence," American Institute of Aeronautics and Astronautics Journal, Vol. 38, No. 4, 2000, pp. 643-656.

[15]Hardin, J. C., and Wang, F. Y., "Sound Generation by Aircraft Wake Vortices," *NASA/CR-2003-212674*, December, 2003.

[16]Howe, M. S., *Theory of Vortex Sound*, Cambridge University Press, Cambridge, U. K., 2003

[17]Inoue, O., "Sound Generation by the Leapfrogging between Two Coaxial Vortex Rings," *Physics of Fluids*, Vol. 14, 2002, pp. 3361-3364.

[18]Inoue, O., Hattori, Y., ad Sasaki, T., "Sound Generation by Coaxial Collision of Two Vortex Rings," *Journal of Fluid Mechanics*, Vol. 424, 2000, pp. 327-365.

[19]Kambe, T., Minota, T., and Takaoka, T., "Oblique Collision of Two Vortex Rings and Its Acoustic Emission," *Phys. Rev. E*, Vol. 48, 1993, pp. 1866-1881.

[20]Kao, H. C., "Body-Vortex Interaction, Sound Generation, and Destructive Interference," *AIAA Journal*, Vol. 40, No. 4, 2002, pp. 652-660.

[21]Knio, O. M., Colorec, L., Juve, D., "Numerical Study of Sound Emission by 2D Regular and Chaotic Vortex Configurations," *Journal of Computational Physics*, Vol. 116, 1995, pp. 226-246.

[22]Kopiev, V. F., and Chernyshev, S. A., "Vortex Ring Eigen-Oscillations as a Source of Sound," *J. Fluid Mech.*, Vol. 341, 1997, pp. 19-57.

[23]Lamb, H., *Hydrodynamics*, Cambridge University Press, Cambridge, U. K. , 7th ed., 1975.

[24]Michel, U. and Bohning, P., "Investigation of Aircraft Wake Vortices with Phased Microphone Arrays," *8th AIAA/CEAS Aeroacoustics Conference*, AIAA Paper No. 2002-2501, Breckenridge, CO, June 2002.

[25]Mitchell, B. E., Lele, S., and Moin, P., "Direct Computation of the Sound from a Compressible Co-Rotating Vortex Pair," *Journal of Fluid Mechanics*, Vol. 285, 1995, pp. 181-202.

[26]Mohring, W., "On Vortex Sound at Low Mach Number," *Journal of Fluid Mechanics*, Vol. 85, 1978, pp. 685-691.

[27]Mohring, W., "Modelling Low Mach Number Noise," in *Mechanics of Sound Generation in Flows*, ed. E.-A. Muller, Springer, 1979.

[28]Muller, B., "On Sound Generation by the Kirchhoff Vortex," Report No. 209/1998, Department of Scientific Computing, Uppsala University, Oct. 1998.

[29]Muller, B., and Yee, H. C., "High Order Numerical Simulation of Sound Generated by the Kirchhoff Vortex," *Computing and Visualization in Science*, Vol. 4, 2002, pp. 197-204.

[30]Powell, A., "Theory of Vortex Sound. *Journal of the Acoustical Society of America*, Vol. 36, 1964, pp. 177-195.

[31]Qiao, W. and Michel, U., "A Study on the Vortex Shedding Noise from the Wake of Aircraft Wings," AIAA Paper No. 2000-1973, Lahaina, HI, June 2000.

[32]Rubin, W. L., "The Generation and Detection of Sound Emitted by Aircraft Wake Vortices in Ground Effect," *J. of Atmospheric and Oceanic Technology*, Vol. 22, May 2005, pp. 543-554.

[33]Saffman, P. G., *Vortex Dynamics*, Cambridge University Press, Cambridge, U. K., 1995.

[34]Tang, S. K., and Ko, N. W. M., "Basic Sound Generation Mechanisms in Inviscid Vortex Interactions at Low Mach Number," *Journal of Sound and Vibration*, Vol. 262, 2003, pp. 87-115.

[35]Tang, S. K., and Ko, N. W. M., "Sound Sources in the Interactions of Two Inviscid Two-Dimensional Vortex Pairs," *Journal of Fluid Mechanics*, Vol. 419, 2000, pp. 87-115.

[36]Wang, F. Y., Wassaf, H. S., Gulsrud, A., Delisi, D. P. and Rudis, R. P., "Acoustic Imaging of Aircraft Wake Vortex Dynamics," AIAA Paper No. 2005-4849, Toronto, Canada, June 2005.

[37]Wassaf, H. S., Ibe, O. C., Dougherty, R. P., and Zhang, Y., "Acoustical Spectral Analysis of a Wake Vortex Cross-Section Using Microphone-Arrays," *Journal of the Acoustical Society of America*, Vol. 117, Issue 4, April 2005, pp. 2546.

[38]Wassaf, H., Hardin, J., and Wang, F., "Atmospheric Effects on Microphone Array Analysis of Aircraft Vortex Sound," AIAA Paper AIAA 2006-2539, *12th AIAA/CEAS Aeroacoustics Conferences*, May 8-10, 2006, Cambridge, MA.

[39]Widnall, S. F., Bliss, D. B., and Tsai, C. Y., "The Instability of Short Wave on a Vortex Ring. *J. Fluid Mech.*, Vol. 66, 1974, pp. 35-47.

[40]Zheng, Z. C., "Far-field Acoustic Pressure from a System of Discrete Vortices with Time-Varying Circulation," AIAA Paper 2005-3005, *11th AIAA/CEAS Aeroacoustics Conference*, May 23-25, 2005, Monterey, CA.

[41]Zheng, Z. C., "Thin-Tube Vortex Simulations for Sinusoidal Instability in a Counter-Rotating Vortex Pair," *International Journal for Numerical Methods in Fluids*, Vol. 39, No. 4, 2002, pp. 301-324.

[42]Zheng, Z. C., and Ash, R. L., "A Study of Aircraft Wake Vortex Behavior Near the Ground," *American Institute of Aeronautics and Astronautics Journal*, Vol. 34, No. 3, 1996, pp. 580-589.

[43]Zheng, Z. C., and Baek, K., "Inviscid Interactions Between Wake Vortices and Shear Layers," *Journal of Aircraft*, Vol. 36, No. 2, 1999, pp. 477-480.

[44]Zheng, Z. C., and Lim, S. H., "Validation and Operation of a Vortex-Wake/Shear Interaction Model," *Journal of Aircraft*, Vol. 37, No. 6, 2000, pp. 1073-1078.